BABAR-CONF-02/01
SLAC-PUB-9153
March, 2002

Improved Measurement of the *CP*-violating Asymmetry Amplitude sin2β

The *BABAR* Collaboration

B. Aubert, D. Boutigny, J.-M. Gaillard, A. Hicheur, Y. Karyotakis, J. P. Lees, P. Robbe, V. Tisserand, and A. Zghiche
Laboratoire de Physique des Particules, F-74941 Annecy-le-Vieux, France

A. Palano and A. Pompili
Università di Bari, Dipartimento di Fisica and INFN, I-70126 Bari, Italy

G. P. Chen, J. C. Chen, N. D. Qi, G. Rong, P. Wang, and Y. S. Zhu
Institute of High Energy Physics, Beijing 100039, China

G. Eigen, I. Ofte, and B. Stugu
University of Bergen, Inst. of Physics, N-5007 Bergen, Norway

G. S. Abrams, A. W. Borgland, A. B. Breon, D. N. Brown, J. Button-Shafer, R. N. Cahn, E. Charles, M. S. Gill, A. V. Gritsan, Y. Groysman, R. G. Jacobsen, R. W. Kadel, J. Kadyk, L. T. Kerth, Yu. G. Kolomensky, J. F. Kral, C. LeClerc, M. E. Levi, G. Lynch, L. M. Mir, P. J. Oddone, M. Pripstein, N. A. Roe, A. Romosan, M. T. Ronan, V. G. Shelkov, A. V. Telnov, and W. A. Wenzel
Lawrence Berkeley National Laboratory and University of California, Berkeley, CA 94720, USA

T. J. Harrison, C. M. Hawkes, D. J. Knowles, S. W. O'Neale, R. C. Penny, A. T. Watson, and N. K. Watson
University of Birmingham, Birmingham, B15 2TT, United Kingdom

T. Deppermann, K. Goetzen, H. Koch, B. Lewandowski, K. Peters, H. Schmuecker, and M. Steinke
Ruhr Universität Bochum, Institut für Experimentalphysik 1, D-44780 Bochum, Germany

N. R. Barlow, W. Bhimji, N. Chevalier, P. J. Clark, W. N. Cottingham, B. Foster, C. Mackay, and F. F. Wilson
University of Bristol, Bristol BS8 1TL, United Kingdom

K. Abe, C. Hearty, T. S. Mattison, J. A. McKenna, and D. Thiessen
University of British Columbia, Vancouver, BC, Canada V6T 1Z1

S. Jolly and A. K. McKemey
Brunel University, Uxbridge, Middlesex UB8 3PH, United Kingdom

V. E. Blinov, A. D. Bukin, D. A. Bukin, A. R. Buzykaev, V. B. Golubev, V. N. Ivanchenko, A. A. Korol, E. A. Kravchenko, A. P. Onuchin, S. I. Serednyakov, Yu. I. Skovpen, and A. N. Yushkov
Budker Institute of Nuclear Physics, Novosibirsk 630090, Russia

D. Best, M. Chao, D. Kirkby, A. J. Lankford, M. Mandelkern, S. McMahon, and D. P. Stoker
University of California at Irvine, Irvine, CA 92697, USA

K. Arisaka, C. Buchanan, and S. Chun
University of California at Los Angeles, Los Angeles, CA 90024, USA

D. B. MacFarlane, S. Prell, Sh. Rahatlou, G. Raven, and V. Sharma

University of California at San Diego, La Jolla, CA 92093, USA

C. Campagnari, B. Dahmes, P. A. Hart, N. Kuznetsova, S. L. Levy,
O. Long, A. Lu, M. A. Mazur, J. D. Richman, and W. Verkerke
University of California at Santa Barbara, Santa Barbara, CA 93106, USA

J. Beringer, A. M. Eisner, M. Grothe, C. A. Heusch, W. S. Lockman, T. Pulliam, T. Schalk,
R. E. Schmitz, B. A. Schumm, A. Seiden, M. Turri, W. Walkowiak, D. C. Williams, and M. G. Wilson
University of California at Santa Cruz, Institute for Particle Physics, Santa Cruz, CA 95064, USA

E. Chen, G. P. Dubois-Felsmann, A. Dvoretskii, D. G. Hitlin, S. Metzler,
J. Oyang, F. C. Porter, A. Ryd, A. Samuel, S. Yang, and R. Y. Zhu
California Institute of Technology, Pasadena, CA 91125, USA

S. Jayatilleke, G. Mancinelli, B. T. Meadows, and M. D. Sokoloff
University of Cincinnati, Cincinnati, OH 45221, USA

T. Barillari, P. Bloom, W. T. Ford, U. Nauenberg, A. Olivas,
P. Rankin, J. Roy, J. G. Smith, W. C. van Hoek, and L. Zhang
University of Colorado, Boulder, CO 80309, USA

J. Blouw, J. L. Harton, M. Krishnamurthy, A. Soffer, W. H. Toki, R. J. Wilson, and J. Zhang
Colorado State University, Fort Collins, CO 80523, USA

T. Brandt, J. Brose, T. Colberg, M. Dickopp, R. S. Dubitzky, A. Hauke, E. Maly,
R. Müller-Pfefferkorn, S. Otto, K. R. Schubert, R. Schwierz, B. Spaan, and L. Wilden
Technische Universität Dresden, Institut für Kern- und Teilchenphysik, D-01062 Dresden, Germany

D. Bernard, G. R. Bonneaud, F. Brochard, J. Cohen-Tanugi,
S. Ferrag, S. T'Jampens, Ch. Thiebaux, G. Vasileiadis, and M. Verderi
Ecole Polytechnique, LLR, F-91128 Palaiseau, France

A. Anjomshoaa, R. Bernet, A. Khan, D. Lavin, F. Muheim, S. Playfer, J. E. Swain, and J. Tinslay
University of Edinburgh, Edinburgh EH9 3JZ, United Kingdom

M. Falbo
Elon University, Elon University, NC 27244-2010, USA

C. Borean, C. Bozzi, and L. Piemontese
Università di Ferrara, Dipartimento di Fisica and INFN, I-44100 Ferrara, Italy

E. Treadwell
Florida A&M University, Tallahassee, FL 32307, USA

F. Anulli,* R. Baldini-Ferroli, A. Calcaterra, R. de Sangro, D. Falciai,
G. Finocchiaro, P. Patteri, I. M. Peruzzi,* M. Piccolo, Y. Xie, and A. Zallo
Laboratori Nazionali di Frascati dell'INFN, I-00044 Frascati, Italy

S. Bagnasco, A. Buzzo, R. Contri, G. Crosetti, M. Lo Vetere, M. Macri, M. R. Monge,
S. Passaggio, F. C. Pastore, C. Patrignani, E. Robutti, A. Santroni, and S. Tosi
Università di Genova, Dipartimento di Fisica and INFN, I-16146 Genova, Italy

M. Morii
Harvard University, Cambridge, MA 02138, USA

R. Bartoldus, R. Hamilton, and U. Mallik
University of Iowa, Iowa City, IA 52242, USA

J. Cochran, H. B. Crawley, J. Lamsa, W. T. Meyer, E. I. Rosenberg, and J. Yi
Iowa State University, Ames, IA 50011-3160, USA

G. Grosdidier, A. Höcker, H. M. Lacker, S. Laplace, F. Le Diberder, V. Lepeltier, A. M. Lutz, S. Plaszczynski, M. H. Schune, S. Trincaz-Duvoid, and G. Wormser
Laboratoire de l'Accélérateur Linéaire, F-91898 Orsay, France

R. M. Bionta, V. Brigljević, D. J. Lange, M. Mugge, K. van Bibber, and D. M. Wright
Lawrence Livermore National Laboratory, Livermore, CA 94550, USA

A. J. Bevan, J. R. Fry, E. Gabathuler, R. Gamet, M. George, M. Kay, D. J. Payne, R. J. Sloane, and C. Touramanis
University of Liverpool, Liverpool L69 3BX, United Kingdom

M. L. Aspinwall, D. A. Bowerman, P. D. Dauncey, U. Egede, I. Eschrich, G. W. Morton, J. A. Nash, P. Sanders, and D. Smith
University of London, Imperial College, London, SW7 2BW, United Kingdom

J. J. Back, G. Bellodi, P. Dixon, P. F. Harrison, R. J. L. Potter, H. W. Shorthouse, P. Strother, and P. B. Vidal
Queen Mary, University of London, E1 4NS, United Kingdom

G. Cowan, S. George, M. G. Green, A. Kurup, C. E. Marker, T. R. McMahon, S. Ricciardi, F. Salvatore, and G. Vaitsas
University of London, Royal Holloway and Bedford New College, Egham, Surrey TW20 0EX, United Kingdom

D. Brown and C. L. Davis
University of Louisville, Louisville, KY 40292, USA

J. Allison, R. J. Barlow, J. T. Boyd, A. C. Forti, F. Jackson, G. D. Lafferty, N. Savvas, J. H. Weatherall, and J. C. Williams
University of Manchester, Manchester M13 9PL, United Kingdom

A. Farbin, A. Jawahery, V. Lillard, J. Olsen, D. A. Roberts, and J. R. Schieck
University of Maryland, College Park, MD 20742, USA

G. Blaylock, C. Dallapiccola, K. T. Flood, S. S. Hertzbach, R. Kofler, V. B. Koptchev, T. B. Moore, H. Staengle, and S. Willocq
University of Massachusetts, Amherst, MA 01003, USA

B. Brau, R. Cowan, G. Sciolla, F. Taylor, and R. K. Yamamoto
Massachusetts Institute of Technology, Laboratory for Nuclear Science, Cambridge, MA 02139, USA

M. Milek and P. M. Patel
McGill University, Montréal, QC, Canada H3A 2T8

F. Palombo and C. Vite
Università di Milano, Dipartimento di Fisica and INFN, I-20133 Milano, Italy

J. M. Bauer, L. Cremaldi, V. Eschenburg, R. Kroeger, J. Reidy, D. A. Sanders, and D. J. Summers
University of Mississippi, University, MS 38677, USA

C. Hast, J. Y. Nief, and P. Taras
Université de Montréal, Laboratoire René J. A. Lévesque, Montréal, QC, Canada H3C 3J7

H. Nicholson
Mount Holyoke College, South Hadley, MA 01075, USA

C. Cartaro, N. Cavallo,† G. De Nardo, F. Fabozzi, C. Gatto, L. Lista, P. Paolucci, D. Piccolo, and C. Sciacca
Università di Napoli Federico II, Dipartimento di Scienze Fisiche and INFN, I-80126, Napoli, Italy

J. M. LoSecco
University of Notre Dame, Notre Dame, IN 46556, USA

J. R. G. Alsmiller and T. A. Gabriel
Oak Ridge National Laboratory, Oak Ridge, TN 37831, USA

J. Brau, R. Frey, E. Grauges, M. Iwasaki, C. T. Potter, N. B. Sinev, and D. Strom
University of Oregon, Eugene, OR 97403, USA

F. Colecchia, F. Dal Corso, A. Dorigo, F. Galeazzi, M. Margoni, M. Morandin, M. Posocco, M. Rotondo, F. Simonetto, R. Stroili, E. Torassa, and C. Voci
Università di Padova, Dipartimento di Fisica and INFN, I-35131 Padova, Italy

M. Benayoun, H. Briand, J. Chauveau, P. David, Ch. de la Vaissière, L. Del Buono, O. Hamon, Ph. Leruste, J. Ocariz, M. Pivk, L. Roos, and J. Stark
Universités Paris VI et VII, Lab de Physique Nucléaire H. E., F-75252 Paris, France

P. F. Manfredi, V. Re, and V. Speziali
Università di Pavia, Dipartimento di Elettronica and INFN, I-27100 Pavia, Italy

E. D. Frank, L. Gladney, Q. H. Guo, and J. Panetta
University of Pennsylvania, Philadelphia, PA 19104, USA

C. Angelini, G. Batignani, S. Bettarini, M. Bondioli, F. Bucci, E. Campagna, M. Carpinelli, F. Forti, M. A. Giorgi, A. Lusiani, G. Marchiori, F. Martinez-Vidal, M. Morganti, N. Neri, E. Paoloni, M. Rama, G. Rizzo, F. Sandrelli, G. Simi, G. Triggiani, and J. Walsh
Università di Pisa, Scuola Normale Superiore and INFN, I-56010 Pisa, Italy

M. Haire, D. Judd, K. Paick, L. Turnbull, and D. E. Wagoner
Prairie View A&M University, Prairie View, TX 77446, USA

J. Albert, P. Elmer, C. Lu, V. Miftakov, S. F. Schaffner, A. J. S. Smith, A. Tumanov, and E. W. Varnes
Princeton University, Princeton, NJ 08544, USA

F. Bellini, G. Cavoto, D. del Re, F. Ferrarotto, F. Ferroni, M. A. Mazzoni, S. Morganti, G. Piredda, M. Serra, and C. Voena
Università di Roma La Sapienza, Dipartimento di Fisica and INFN, I-00185 Roma, Italy

R. Faccini
University of California at San Diego, La Jolla, CA 92093, USA and
Università di Roma La Sapienza, Dipartimento di Fisica and INFN, I-00185 Roma, Italy

S. Christ and R. Waldi
Universität Rostock, D-18051 Rostock, Germany

T. Adye, N. De Groot, B. Franek, N. I. Geddes, G. P. Gopal, and S. M. Xella
Rutherford Appleton Laboratory, Chilton, Didcot, Oxon, OX11 0QX, United Kingdom

R. Aleksan, S. Emery, A. Gaidot, S. F. Ganzhur, P.-F. Giraud, G. Hamel de Monchenault, W. Kozanecki, M. Langer, G. W. London, B. Mayer, B. Serfass, G. Vasseur, Ch. Yèche, and M. Zito
DAPNIA, Commissariat à l'Energie Atomique/Saclay, F-91191 Gif-sur-Yvette, France

M. V. Purohit, A. W. Weidemann, and F. X. Yumiceva
University of South Carolina, Columbia, SC 29208, USA

I. Adam, D. Aston, N. Berger, A. M. Boyarski, G. Calderini, M. R. Convery, D. P. Coupal, D. Dong, J. Dorfan, W. Dunwoodie, R. C. Field, T. Glanzman, S. J. Gowdy, T. Haas, T. Hadig,

V. Halyo, T. Himel, T. Hryn'ova, M. E. Huffer, W. R. Innes, C. P. Jessop, M. H. Kelsey, P. Kim, M. L. Kocian, U. Langenegger, D. W. G. S. Leith, S. Luitz, V. Luth, H. L. Lynch, H. Marsiske, S. Menke, R. Messner, D. R. Muller, C. P. O'Grady, V. E. Ozcan, A. Perazzo, M. Perl, S. Petrak, H. Quinn, B. N. Ratcliff, S. H. Robertson, A. Roodman, A. A. Salnikov, T. Schietinger, R. H. Schindler, J. Schwiening, A. Snyder, A. Soha, S. M. Spanier, J. Stelzer, D. Su, M. K. Sullivan, H. A. Tanaka, J. Va'vra, S. R. Wagner, M. Weaver, A. J. R. Weinstein, W. J. Wisniewski, D. H. Wright, and C. C. Young
Stanford Linear Accelerator Center, Stanford, CA 94309, USA

P. R. Burchat, C. H. Cheng, T. I. Meyer, and C. Roat
Stanford University, Stanford, CA 94305-4060, USA

R. Henderson
TRIUMF, Vancouver, BC, Canada V6T 2A3

W. Bugg and H. Cohn
University of Tennessee, Knoxville, TN 37996, USA

J. M. Izen, I. Kitayama, and X. C. Lou
University of Texas at Dallas, Richardson, TX 75083, USA

F. Bianchi, M. Bona, and D. Gamba
Università di Torino, Dipartimento di Fisica Sperimentale and INFN, I-10125 Torino, Italy

L. Bosisio, G. Della Ricca, S. Dittongo, L. Lanceri, P. Poropat, L. Vitale, and G. Vuagnin
Università di Trieste, Dipartimento di Fisica and INFN, I-34127 Trieste, Italy

R. S. Panvini
Vanderbilt University, Nashville, TN 37235, USA

C. M. Brown, P. D. Jackson, R. Kowalewski, and J. M. Roney
University of Victoria, Victoria, BC, Canada V8W 3P6

H. R. Band, S. Dasu, M. Datta, A. M. Eichenbaum, H. Hu, J. R. Johnson, R. Liu, F. Di Lodovico, Y. Pan, R. Prepost, I. J. Scott, S. J. Sekula, J. H. von Wimmersperg-Toeller, S. L. Wu, and Z. Yu
University of Wisconsin, Madison, WI 53706, USA

T. M. B. Kordich and H. Neal
Yale University, New Haven, CT 06511, USA

(Dated: February 7, 2008)

We present updated results on time-dependent *CP*-violating asymmetries in neutral B decays to several *CP* eigenstates. The measurements use a data sample of about 62 million $\Upsilon(4S) \to B\overline{B}$ decays collected between 1999 and 2001 by the *BABAR* detector at the PEP-II asymmetric-energy B Factory at SLAC. In this sample we study events in which one neutral B meson is fully reconstructed in a final state containing a charmonium meson and the flavor of the other neutral B meson is determined from its decay products. The amplitude of the *CP*-violating asymmetry, which in the Standard Model is proportional to $\sin 2\beta$, is derived from the decay time distributions in such events. We measure $\sin 2\beta = 0.75 \pm 0.09$ (stat) ± 0.04 (syst) and $|\lambda| = 0.92 \pm 0.06$ (stat) ± 0.02 (syst). The latter is consistent with the Standard Model expectation of no direct *CP* violation. These results are preliminary.

PACS numbers: 13.25.Hw, 12.15.Hh, 11.30.Er

The Standard Model of electroweak interactions describes *CP* violation in weak decays as a consequence of a

*Also with Università di Perugia, I-06100 Perugia, Italy
†Also with Università della Basilicata, I-85100 Potenza, Italy

complex phase in the three-generation Cabibbo-Kobayashi-Maskawa [1] (CKM) quark-mixing matrix. In this picture, measurements of *CP*-violating asymmetries in the time distributions of B^0 decays to charmonium final states provide a direct measurement of $\sin 2\beta$ [2], where $\beta \equiv \arg\left[-V_{\rm cd}V_{\rm cb}^*/V_{\rm td}V_{\rm tb}^*\right]$.

Measurements of the *CP*-violating asymmetry parameter $\sin 2\beta$ have recently been published by the *BABAR* [3] and Belle [4] collaborations from data taken between 1999 and summer 2001 at the PEP-II and KEKB asymmetric-energy e^+e^- colliders. These results, which followed less precise measurements [5], established *CP* violation in the B^0 system. In this paper, we report an updated measurement of $\sin 2\beta$, using a sample of 62 million B^0 decays collected with the *BABAR* detector. Since our previous measurement, we have added a sample of 30 million B^0 decays collected in the latter half of 2001, and have improved data reconstruction and analysis techniques. The measurement technique is described in detail in Ref. [6]. The discussion here is limited to the changes in the analysis with respect to the published results [3, 6].

Since the *BABAR* detector is described in detail elsewhere [7], only a brief description is given here. Surrounding the beam-pipe is a silicon vertex tracker (SVT), which provides precise measurements of the trajectories of charged particles as they leave the e^+e^- interaction point. Outside of the SVT, a 40-layer drift chamber (DCH) allows measurements of track momenta in a 1.5 T magnetic field as well as energy-loss measurements, which contribute to charged particle identification. Surrounding the DCH is a detector of internally reflected Cherenkov radiation (DIRC), which provides charged hadron identification. Outside of the DIRC is a CsI(Tl) electromagnetic calorimeter (EMC) that is used to detect photons, provide electron identification and reconstruct neutral hadrons. The EMC is surrounded by a superconducting coil, which creates the magnetic field for momentum measurements. Outside of the coil, the flux return is instrumented with resistive plate chambers interspersed with iron (IFR) for the identification of muons and long-lived neutral hadrons. We use the GEANT4 [8] software to simulate interactions of particles traversing the *BABAR* detector.

From approximately 56 fb^{-1} of data recorded at the $\Upsilon(4S)$ resonance, corresponding to 62 million produced $B\overline{B}$ pairs, we reconstruct a sample of neutral B mesons, B_{CP}, decaying to the final states $J/\psi K^0_S$ ($K^0_S \to \pi^+\pi^-,\ \pi^0\pi^0$), $\psi(2S)K^0_S$ ($K^0_S \to \pi^+\pi^-$), $\chi_{c1}K^0_S$ ($K^0_S \to \pi^+\pi^-$), $J/\psi K^{*0}$ ($K^{*0} \to K^0_S\pi^0,\ K^0_S \to \pi^+\pi^-$), and $J/\psi K^0_L$. The J/ψ and $\psi(2S)$ mesons are reconstructed through their decays to e^+e^- and $\mu^+\mu^-$; the $\psi(2S)$ is also reconstructed through its decay to $J/\psi\pi^+\pi^-$. The χ_{c1} meson is reconstructed in the decay mode $J/\psi\gamma$. We examine each of the events in the B_{CP} sample for evidence that the recoiling neutral B meson decayed as a B^0 or $\overline{B}^0$ (flavor tag).

The decay-time distribution of B decays to a *CP* eigenstate with a B^0 or $\overline{B}^0$ tag can be expressed in terms of a complex parameter λ that depends on both the B^0-$\overline{B}^0$ oscillation amplitude and the amplitudes describing $\overline{B}^0$ and B^0 decays to this final state [9]. The decay rate $\mathrm{f}_+(\mathrm{f}_-)$ when the tagging meson is a $B^0(\overline{B}^0)$ is given by

$$\mathrm{f}_\pm(\Delta t) = \frac{e^{-|\Delta t|/\tau_{B^0}}}{4\tau_{B^0}} \times \left[1 \pm \frac{2\,\mathcal{I}m\lambda}{1+|\lambda|^2}\sin(\Delta m_d \Delta t) \mp \frac{1-|\lambda|^2}{1+|\lambda|^2}\cos(\Delta m_d \Delta t)\right], \tag{1}$$

where $\Delta t = t_{\rm rec} - t_{\rm tag}$ is the difference between the proper decay time of the reconstructed B meson ($B_{\rm rec}$) and the proper decay time of the tagging B meson ($B_{\rm tag}$), τ_{B^0} is the B^0 lifetime, Δm_d is the mass difference determined from B^0-$\overline{B}^0$ oscillations, and the lifetime difference between the neutral B mass eigenstates is assumed to be negligible. The sine term in Eq. 1 is due to the interference between direct decay and decay after flavor change, and the cosine term is due to the interference between two or more decay amplitudes with different weak phases. Evidence for *CP* violation can be observed as a difference between the Δt distributions of B^0- and $\overline{B}^0$-tagged events or as an asymmetry with respect to $\Delta t = 0$ for either flavor tag.

In the Standard Model, $\lambda = \eta_f e^{-2i\beta}$ for charmonium-containing $b \to c\bar{c}s$ decays where η_f is the *CP* eigenvalue of the final state f. Thus, the time-dependent *CP*-violating asymmetry is

$$A_{CP}(\Delta t) \equiv \frac{\mathrm{f}_+(\Delta t) - \mathrm{f}_-(\Delta t)}{\mathrm{f}_+(\Delta t) + \mathrm{f}_-(\Delta t)} = -\eta_f \sin 2\beta \sin(\Delta m_d\,\Delta t), \tag{2}$$

with $\eta_f = -1$ for $J/\psi K^0_S$, $\psi(2S)K^0_S$, and $\chi_{c1}K^0_S$, and $+1$ for $J/\psi K^0_L$.

The measurement of $\sin 2\beta$ with the decay mode $B \to J/\psi K^{*0}(K^{*0} \to K^0_S\pi^0)$ is experimentally complicated by the presence of both even (L=0, 2) and odd (L=1) orbital angular momenta in the final state. With the measured *CP*-even and *CP*-odd contributions to the decay rate [10], the experimental sensitivity to $\sin 2\beta$ is reduced by 24% compared to pure *CP* eigenstates. The interference between *CP*-even and *CP*-odd amplitudes in this mode allows a measurement of $\cos 2\beta$ up to a sign ambiguity. The time- and angle-dependent decay rate $\mathrm{f}_+(\mathrm{f}_-)$ when the tagging meson is a $B^0(\overline{B}^0)$ is given by

$$\mathrm{f}_{\pm}(\Delta t,\vec{\omega}) \;=\; \frac{e^{-|\Delta t|/\tau_{B^0}}}{4\tau_{B^0}}\Big[I(\vec{\omega};\vec{\mathcal{A}}) \mp \Big\{C(\vec{\omega};\vec{\mathcal{A}})\cos(\Delta m_d\Delta t) + \Big[S_{\sin 2\beta}(\vec{\omega};\vec{\mathcal{A}})\sin 2\beta + S_{\cos 2\beta}(\vec{\omega};\vec{\mathcal{A}})\cos 2\beta\Big]\sin(\Delta m_d\Delta t)\Big\}\Big] \tag{3}$$

where the coefficients I, C, $S_{\sin 2\beta}$, and $S_{\cos 2\beta}$ are functions of three transversity angles $\vec{\omega}$ and the previously measured transversity amplitudes $\vec{\mathcal{A}}$ [10] (see appendix A).

The event selection, lepton and charged kaon identification, and J/ψ and $\psi(2S)$ reconstruction used in this analysis are similar to those described in Ref. [3, 6]. Since these earlier publications, significant improvements have been made in the analysis. Charged kaon identification has improved due to a better alignment of the Cherenkov detector and better Cherenkov angle reconstruction. For the $B^0 \to J/\psi K^0_L$ selection, we have loosened the muon selection requirements for $J/\psi \to \mu^+\mu^-$ and the π^0 veto for K^0_L candidates. In the $K^0_S \to \pi^+\pi^-$ selection for $B^0 \to J/\psi K^0_S$ candidates, the requirement on the $\pi^+\pi^-$ mass has been relaxed to $472 < m(\pi^+\pi^-) < 522\,\mathrm{MeV}/c^2$. We have increased the sensitivity to $\sin 2\beta$ for the mode $J/\psi K^{*0}(K^{*0} \to K^0_S\pi^0)$ by taking into account the transversity angles for each event instead of integrating out the angle dependence. Events reconstructed in this mode that have a candidate in the mode $J/\psi K^{*+}(K^{*+} \to K^0_S\pi^+)$ are rejected. In addition, the whole dataset has been processed with a uniform reconstruction algorithm and detector calibration. This provides, in particular, better alignment of the tracking system and improved track reconstruction efficiency for the 20 fb^{-1} of data collected in 1999–2000. For example, the event yield increased by 11% (37%) for the $\eta_f = -1$ ($J/\psi K^0_L$) sample while the purity only decreased by 4% (3%). The effect of all improvements decreases the error on $\sin 2\beta$ scaled to the same integrated luminosity by 13%.

Candidates in the B_{CP} sample are selected by requiring that the difference ΔE between their energy and the beam energy in the center-of-mass frame be less than three standard deviations from zero. For modes involving K^0_S, the beam-energy substituted mass $m_{\mathrm{ES}} = \sqrt{(E^{\mathrm{cm}}_{\mathrm{beam}})^2 - (p^{\mathrm{cm}}_B)^2}$ must be greater than $5.2\,\mathrm{GeV}/c^2$. The resolution for ΔE is about 10 MeV, except for the $K^0_S \to \pi^0\pi^0$ (33 MeV), the $J/\psi K^{*0}$ (20 MeV) and the $J/\psi K^0_L$ (3.5 MeV after B mass constraint) modes. For the purpose of determining numbers of events and purities, a signal region $5.270\ (5.273) < m_{\mathrm{ES}} < 5.290\ (5.288)\,\mathrm{GeV}/c^2$ is used for modes containing K^0_S (K^{*0}). The signal region for the mode $J/\psi K^0_L$ is defined by $|\Delta E| < 10\,\mathrm{MeV}$.

A measurement of A_{CP} requires a determination of the experimental Δt resolution and the fraction of events in which the tag assignment is incorrect. A mistag fraction w reduces the observed CP asymmetry by a factor $(1-2w)$. Mistag fractions and Δt resolution functions are determined from a sample B_{flav} of neutral B decays to flavor eigenstates consisting of the channels $D^{(*)-}h^+(h^+ = \pi^+, \rho^+,$ and $a_1^+)$ and $J/\psi K^{*0}(K^{*0} \to K^+\pi^-)$. Validation studies are performed with a control sample of charged B mesons decaying to the final states $J/\psi K^{(*)+}$, $\psi(2S)K^+$, $\chi_{c1}K^+$, and $D^{(*)0}\pi^+$.

The methods for flavor tagging and vertex reconstruction, and the determination of Δt, are described in Ref. [6]. For flavor tagging, we exploit information from the recoil B decay in the event. The charges of energetic electrons and muons from semileptonic B decays, kaons, soft pions from D^* decays, and high momentum particles are correlated with the flavor of the decaying b quark. For example, a positive lepton indicates a B^0 tag. About 68% of the events can be assigned to one of four hierarchical, mutually exclusive tagging categories. The remaining untagged events are excluded from further analysis.

For a lepton tag we require an electron or muon candidate with a center-of-mass momentum $p_{\mathrm{cm}} > 1.0$ or $1.1\,\mathrm{GeV}/c$, respectively. This efficiently selects primary leptons from semileptonic B decays and reduces contamination due to oppositely-charged leptons from charm decays. Events satisfying these criteria are assigned to the `Lepton` category unless the lepton charge and the net charge of all kaon candidates indicate opposite flavor tags. Events without a lepton tag but with a non-zero net kaon charge are assigned to the `Kaon` category. All remaining events are passed to a neural network algorithm whose main inputs are the momentum and charge of the track with the highest center-of-mass momentum, and the outputs of secondary networks, trained with Monte Carlo samples to identify primary leptons, kaons, and soft pions. Based on the output of the neural network algorithm, events are tagged as B^0 or $\overline{B}^0$ and assigned to the `NT1` (more certain tags) or `NT2` (less certain tags) category, or not tagged at all. The tagging power of the `NT1` and `NT2` categories arises primarily from soft pions and from recovering unidentified isolated primary electrons and muons.

The time interval Δt between the two B decays is calculated from the measured separation Δz between the decay vertex of the reconstructed B meson (B_{rec}) and the vertex of the flavor-tagging B meson (B_{tag}) along the z axis. The calculation of Δt includes an event-by-event correction for the direction of the B_{rec} with respect to the z direction in the $\Upsilon(4S)$ frame. We determine the z position of the B_{rec} vertex from the charged tracks that constitute the B_{rec} candidate. The decay vertex of the B_{tag} is determined by fitting the tracks not belonging to the B_{rec} candidate to a

common vertex. An additional constraint on the tagging vertex comes from a pseudotrack computed from the $B_{\rm rec}$ vertex and three-momentum, the beam-spot (with a vertical size of 10 μm), and the $\Upsilon(4S)$ momentum. For 99.5% of the reconstructed events the r.m.s. Δz resolution is 180 μm. An accepted candidate must have converged fits for the $B_{\rm rec}$ and $B_{\rm tag}$ vertices, a Δt error less than 2.5 ps, and a measured $|\Delta t| < 20$ ps. The fraction of events in data satisfying these requirements is 93%.

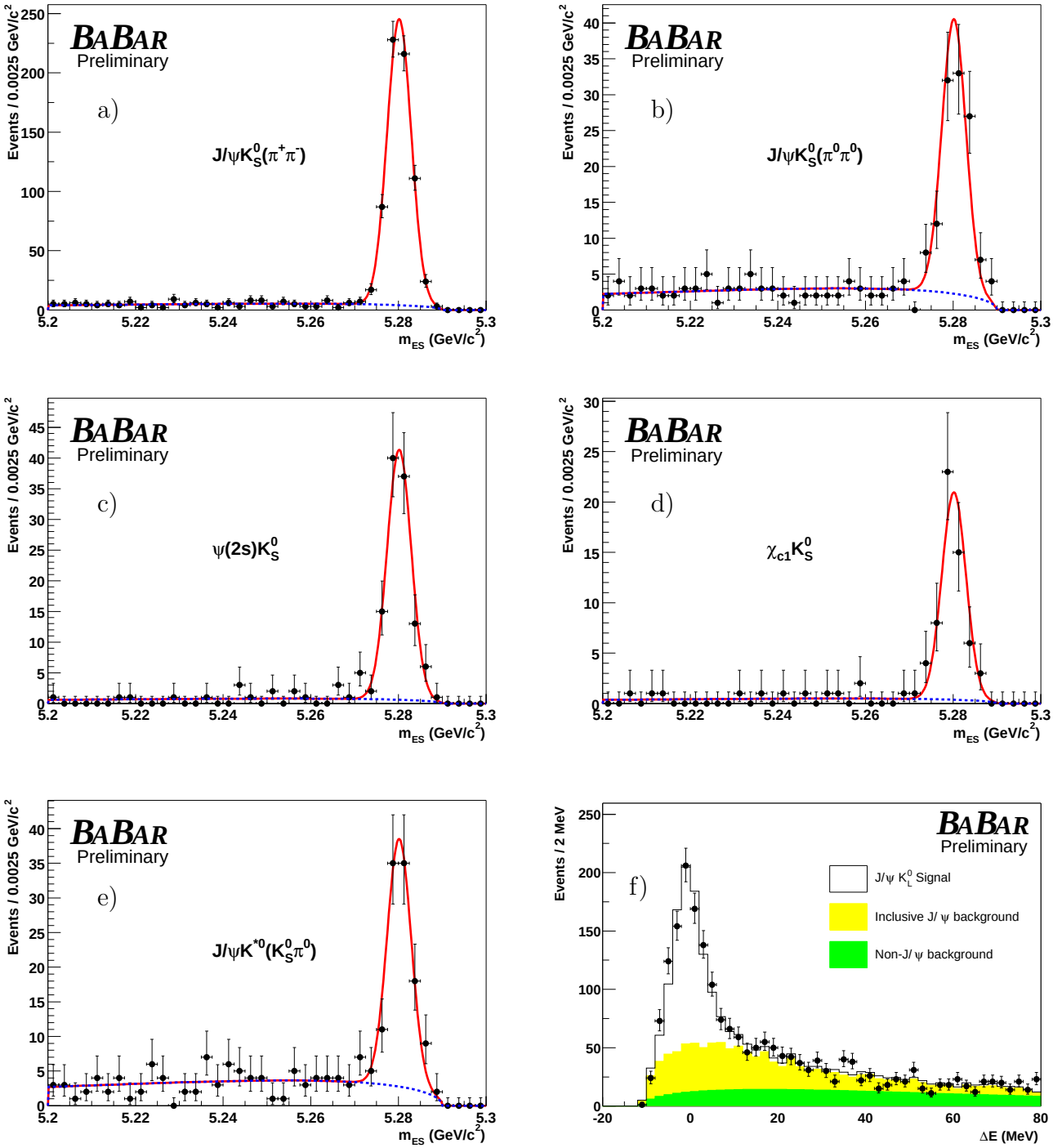

FIG. 1: Distribution of $m_{\rm ES}$ for flavor tagged B_{CP} candidates selected in the final states a) $J/\psi K^0_S$ ($K^0_S \to \pi^+\pi^-$), b) $J/\psi K^0_S$ ($K^0_S \to \pi^0\pi^0$), c) $\psi(2S)K^0_S$, d) $\chi_{c1}K^0_S$, e) $J/\psi K^{*0}(K^{*0} \to K^0_S\pi^0)$, and f) distribution of ΔE for flavor tagged $J/\psi\, K^0_L$ candidates.

In Table I we list the numbers of events and the signal purities for the tagged B_{CP} candidates. The purities are determined from fits to the $m_{\rm ES}$ (all K^0_S modes except $J/\psi K^{*0}$) or ΔE (K^0_L mode) distributions in data, or from Monte Carlo simulation ($J/\psi K^{*0}$ mode). Figure 1 shows the $m_{\rm ES}$ distributions for modes containing a K^0_S, and ΔE for the $J/\psi\ K^0_L$ candidates. For modes containing a K^0_S, we use a Monte Carlo simulation to estimate the fractions of events in the signal peaks that are due to cross-feed from other decay modes. The fractions of peaking background range between $(0.8 \pm 0.2)\%$ for $J/\psi K^0_S$ ($K^0_S \to \pi^+\pi^-$) and $(6.0 \pm 1.8)\%$ for $\psi(2S)K^0_S$. For the $J/\psi K^0_L$ decay mode, the composition, effective η_f, and ΔE distributions of the individual background sources are determined either from Monte Carlo simulation (for B decays to J/ψ) or from the $m_{\ell^+\ell^-}$ sidebands in data (for fake $J/\psi \to \ell^+\ell^-$). The tagging efficiencies for the four tagging categories are measured from data and summarized in Table II.

TABLE I: Number of tagged events, signal purity, and result of fitting for *CP* asymmetries in the full *CP* sample and in various subsamples, as well as in the $B_{\rm flav}$ and charged B control samples. Purity is the fitted number of signal events divided by the total number of events in the ΔE and $m_{\rm ES}$ signal region defined in the text. Errors are statistical only.

Sample	$N_{\rm tag}$	Purity (%)	sin2β
Full *CP* sample	1850	79	0.75 ± 0.09
$J/\psi K^0_S$ ($K^0_S \to \pi^+\pi^-$)	693	96	0.79 ± 0.11
$J/\psi K^0_S$ ($K^0_S \to \pi^0\pi^0$)	123	89	0.42 ± 0.33
$\psi(2S)K^0_S$	119	89	0.84 ± 0.32
$\chi_{c1}K^0_S$	60	94	0.84 ± 0.49
$J/\psi K^0_L$	742	57	0.73 ± 0.19
$J/\psi K^{*0}$ ($K^{*0} \to K^0_S\pi^0$)	113	83	0.62 ± 0.56
$J/\psi K^0_S$, $\psi(2S)K^0_S$, $\chi_{c1}K^0_S$ only ($\eta_f = -1$)	995	94	0.76 ± 0.10
`Lepton` tags	176	97	0.73 ± 0.16
`Kaon` tags	504	95	0.75 ± 0.14
`NT1` tags	117	95	0.86 ± 0.33
`NT2` tags	198	94	0.84 ± 0.61
B^0 tags	471	94	0.79 ± 0.14
$\overline{B}^0$ tags	524	95	0.73 ± 0.14
$B_{\rm flav}$ sample	17546	85	0.00 ± 0.03
Charged B sample	14768	89	−0.02 ± 0.03

TABLE II: Average mistag fractions w_i and mistag differences $\Delta w_i = w_i(B^0) - w_i(\overline{B}^0)$, extracted for each tagging category i from the maximum-likelihood fit to the time distribution for the fully-reconstructed B^0 sample ($B_{\rm flav}$ and B_{CP}). The figure of merit for tagging is the effective tagging efficiency $Q_i = \varepsilon_i(1-2w_i)^2$, where ε_i is the fraction of events with a reconstructed tag vertex that is assigned to the i^{th} category. Uncertainties are statistical only. The statistical error on sin2β is proportional to $1/\sqrt{Q}$, where $Q = \sum Q_i$.

Category	ε (%)	w (%)	Δw (%)	Q (%)
`Lepton`	11.1 ± 0.2	8.6 ± 0.9	0.6 ± 1.5	7.6 ± 0.4
`Kaon`	34.7 ± 0.4	18.1 ± 0.7	−0.9 ± 1.1	14.1 ± 0.6
`NT1`	7.7 ± 0.2	22.0 ± 1.5	1.4 ± 2.3	2.4 ± 0.3
`NT2`	14.0 ± 0.3	37.3 ± 1.3	−4.7 ± 1.9	0.9 ± 0.2
All	67.5 ± 0.5			25.1 ± 0.8

We determine sin2β with a simultaneous unbinned maximum likelihood fit to the Δt distributions of the B_{CP} and $B_{\rm flav}$ tagged samples. Equations 1 (with $|\lambda| = 1$) and 3 describe the Δt distribution of the $\eta_f = -1$ and $J/\psi\ K^0_L$ samples, and the $J/\psi\ K^{*0}$ sample, respectively. The Δt distributions of the $B_{\rm flav}$ sample evolve according to the known frequency for flavor oscillation in neutral B mesons. The observed amplitudes for the *CP* asymmetry in the B_{CP} sample and for flavor oscillation in the $B_{\rm flav}$ sample are reduced by the same factor $(1-2w)$ due to mistags. The Δt distributions for the B_{CP} and $B_{\rm flav}$ samples are both convolved with a common Δt resolution function. Events are assigned signal and background probabilities based on the $m_{\rm ES}$ (all modes except $J/\psi K^0_L$) or ΔE ($J/\psi K^0_L$) distributions. Backgrounds are incorporated with an empirical description of their Δt evolution, containing prompt and non-prompt components convolved with a separate resolution function [6].

The Δt resolution function $\mathcal{R}$ for the signal is represented in terms of $\delta_t \equiv \Delta t - \Delta t_{\rm true}$ by a sum of three Gaussian distributions with different means and widths:

$$\mathcal{R}(\delta_{\rm t}) \;=\; \sum_{k=\rm core,tail} \frac{f_k}{S_k\sigma_{\Delta t}\sqrt{2\pi}} \exp\left(-\frac{(\delta_{\rm t}-b_k\sigma_{\Delta t})^2}{2(S_k\sigma_{\Delta t})^2}\right) + \frac{f_{\rm outlier}}{\sigma_{\rm outlier}\sqrt{2\pi}} \exp\left(-\frac{\delta_{\rm t}^2}{2{\sigma_{\rm outlier}}^2}\right). \tag{4}$$

For the core and tail Gaussians, we use two separate scale factors $S_{\rm core}$ and $S_{\rm tail}$ to multiply the measurement uncertainty $\sigma_{\Delta t}$ that is derived from the vertex fit for each event. The scale factor for the tail component $S_{\rm tail}$ is fixed to the value found in Monte Carlo simulation since it is strongly correlated with the other resolution function parameters. The core and tail Gaussian distributions are allowed to have nonzero means to account for any daughters of long-lived charm particles included in the $B_{\rm tag}$ vertex. In the resolution function, mean offsets b_k are multiplied by the event-by-event measurement uncertainty $\sigma_{\Delta t}$ to account for an observed correlation between the mean of the $\delta_{\rm t}$ distribution and the measurement uncertainty $\sigma_{\Delta t}$ in Monte Carlo simulation. The mean of the core Gaussian is allowed to be different for each tagging category. One common mean is used for the tail component. The outlier Gaussian has a fixed width and no offset; it accounts for the fewer than 0.5% of events with incorrectly reconstructed vertices. In simulated events, we find no significant difference between the Δt resolution function of the B_{CP} sample and of the $B_{\rm flav}$ sample. This is expected, since the $B_{\rm tag}$ vertex precision dominates the Δt resolution. Hence, the same resolution function is used for all modes.

TABLE III: Δt resolution function parameters for $B_{\rm flav}$ and B_{CP} candidates extracted from the simultaneous maximum-likelihood fit to the Δt distributions for the $B_{\rm flav}$ and B_{CP} samples.

$S_{\rm core}$	1.19 ± 0.07	$S_{\rm tail}$	3.0 (fixed)
$b_{\rm core}$ (`lepton`)	0.01 ± 0.07	$b_{\rm tail}$	-2.5 ± 1.7
$b_{\rm core}$ (`kaon`)	-0.24 ± 0.04	$\sigma_{\rm outlier}$	8 ps (fixed)
$b_{\rm core}$ (`NT1`)	-0.20 ± 0.08	$f_{\rm tail}$	0.05 ± 0.04
$b_{\rm core}$ (`NT2`)	-0.21 ± 0.06	$f_{\rm outlier}$	0.004 ± 0.002

A total of 35 parameters are varied in the final fit, including the values of sin2β (1), the average mistag fraction w and the difference Δw between B^0 and $\overline{B}^0$ mistags for each tagging category (8), parameters for the signal Δt resolution (8), and parameters for background time dependence (6), Δt resolution (3), and mistag fractions (8). In addition, we allow cos2β (1), which is determined from the $J/\psi K^{*0}$ events, to vary in the fit. The sign of cos2β cannot be determined due to a twofold ambiguity in the relative strong phases of the angular amplitudes [11]. We use the convention for the strong phases given in Appendix A.

The determination of the mistag fractions and Δt resolution function for the signal is dominated by the high-statistics $B_{\rm flav}$ sample. The measured mistag fractions and the parameters of the signal resolution function are listed in Tables II and III. Background parameters are determined from events with $m_{\rm ES} < 5.27\,{\rm GeV}/c^2$ (except $J/\psi K^0_L$ and $J/\psi K^{*0}$). We fix $\tau_{B^0} = 1.548\,{\rm ps}$ and $\Delta m_d = 0.472\,{\rm ps}^{-1}$ [12]. The largest correlation between sin2β and any linear combination of the other free parameters is 0.14.

The simultaneous fit to all *CP* decay modes and the flavor decay modes yields

$$\sin2\beta = 0.75 \pm 0.09\ ({\rm stat}) \pm 0.04\ ({\rm syst}).$$

Figure 2 shows the Δt distributions and asymmetries in yields between B^0 tags and $\overline{B}^0$ tags for the $\eta_f = -1$ and $\eta_f = +1$ samples as a function of Δt, overlaid with the projection of the global likelihood fit result.

Repeating the fit with all parameters except sin2β fixed to their values at the global maximum likelihood, we attribute a total contribution in quadrature of 0.01 to the error on sin2β due to the combined statistical uncertainties in mistag rates, Δt resolution, and background parameters. The dominant sources of systematic error are due to uncertainties in the level, composition, and *CP* asymmetry of the background in the selected *CP* events (0.022), limited Monte Carlo simulation statistics (0.014), and the assumed parameterization of the Δt resolution function (0.013), due in part to residual uncertainties in the SVT alignment. Uncertainties in Δm_d and τ_{B^0} each contribute 0.010 to the systematic error. We have performed fits with Δm_d and τ_{B^0} fixed to a series of values around the corresponding world averages in order to determine the dependence of sin2β on these two parameters and find that $\sin2\beta = [0.75 - 0.31(\Delta m_d - 0.472\ {\rm ps}^{-1}) - 0.62(\tau_{B^0} - 1.548\ {\rm ps})]$.

The large sample of reconstructed events allows a number of consistency checks, including separation of the data by decay mode, tagging category, and $B_{\rm tag}$ flavor. The results of fits to these subsamples for the $\eta_f = -1$ sample are shown in Table I and found to be statistically consistent. The fit results to the samples of non-*CP* decay modes indicate no statistically significant asymmetry. The distributions and asymmetry in yields for B^0 and $\overline{B}^0$ tags as a function of Δt for the $B_{\rm flav}$ sample are shown in Fig. 3. In addition, we have made a number of detailed analyses of the

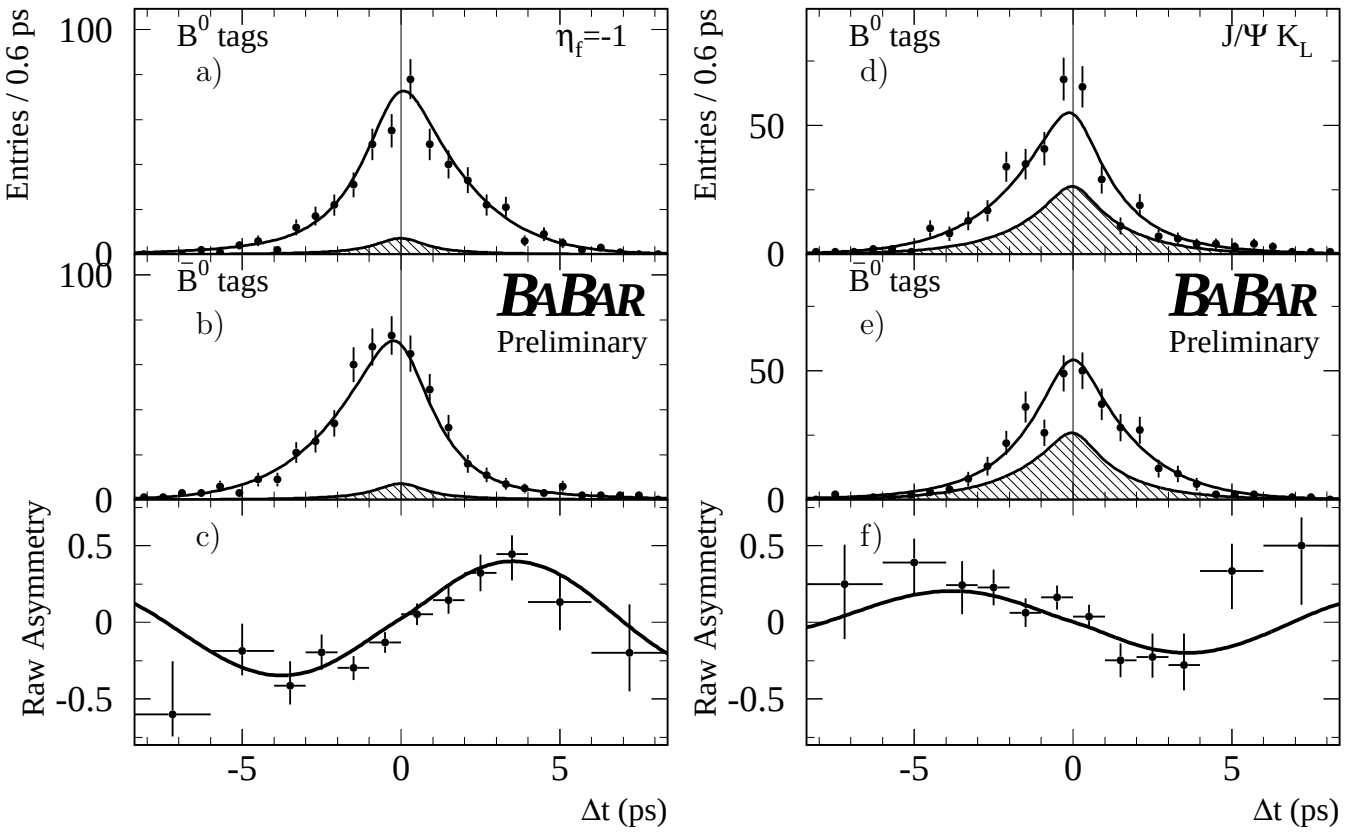

FIG. 2: Number of $\eta_f = -1$ candidates ($J/\psi K^0_S$, $\psi(2S)K^0_S$, $\chi_{c1}K^0_S$) in the signal region a) with a B^0 tag N_{B^0} and b) with a $\overline{B}^0$ tag $N_{\overline{B}^0}$, and c) the raw asymmetry $(N_{B^0} - N_{\overline{B}^0})/(N_{B^0} + N_{\overline{B}^0})$, as functions of Δt. The solid curves represent the result of the combined fit to the full $B_{\rm CP}$ sample. The shaded regions represent the background contributions. Figures d) – f) contain the corresponding information for the $\eta_f = +1$ mode $J/\psi K^0_L$. The likelihood is normalized to the total number of B^0 and $\overline{B}^0$ tags. The value of sin2β is independent of the individual normalizations and therefore of the difference between the number of B^0 and $\overline{B}^0$ tags. This difference is responsible for the small vertical shift between the data points and the solid curves.

expected distribution of changes in sin2β that might result from reprocessing, in order to account for the correlations between the two results from the same sample. From these studies, we conclude that the observed difference in the 1999–2000 result, before and after reprocessing, is equivalent to about two standard deviations of the distribution of predicted changes due to reprocessing for events that appear in common. The change in the overall result in the 1999–2000 dataset, from sin2$\beta = 0.45 \pm 0.20$ to 0.60 ± 0.15, is consistent with the effects of both reprocessing and event selection modifications.

With the theoretically preferred choice of the strong phases, consistent with the hypothesis of the s-quark helicity conservation in the decay [13], the parameter cos2β is measured to be $+3.3^{+0.6}_{-1.0}$ (stat)$^{+0.6}_{-0.7}$ (syst). This value is 2.2 σ away from the one obtained using the relation $\sqrt{1-\sin^2 2\beta} = 0.66$. The dominant contributions to the systematic error on cos2β are due to uncertainties in the transversity amplitudes for the signal ($^{-0.4}_{+0.2}$) and the background (± 0.5). If we fix cos2β to 0.66, the measured value of sin2β does not change. For the alternative set of strong phases, $(\phi_\perp,\ \phi_\parallel) \rightarrow (\pi - \phi_\perp,\ -\phi_\parallel)$, the sign of cos2$\beta$ flips, yielding cos2$\beta = -3.3^{+1.0}_{-0.6}$ (stat)$^{+0.7}_{-0.6}$ (syst).

If the parameter $|\lambda|$ in Eq. 1 is allowed to float in the fit to the $\eta_f = -1$ sample, which has high purity and requires minimal assumptions on the effect of backgrounds, the value obtained is $|\lambda| = 0.92 \pm 0.06$ (stat) ± 0.02 (syst). The sources of the systematic error are the same as for the sin2β measurement with an additional contribution in quadrature of 0.012 from the uncertainty on the difference in the tagging efficiencies for B^0 and $\overline{B}^0$ tagged events. In this fit, the coefficient of the sin($\Delta m_d \Delta t$) term in Eq. 1 is measured to be 0.76 ± 0.10 (stat) in agreement with Table I.

This analysis supersedes our previous result [3]. It provides the single most precise measurement of sin2β currently available and is consistent with the range implied by measurements and theoretical estimates of the magnitudes of CKM matrix elements in the context of the Standard Model [14].

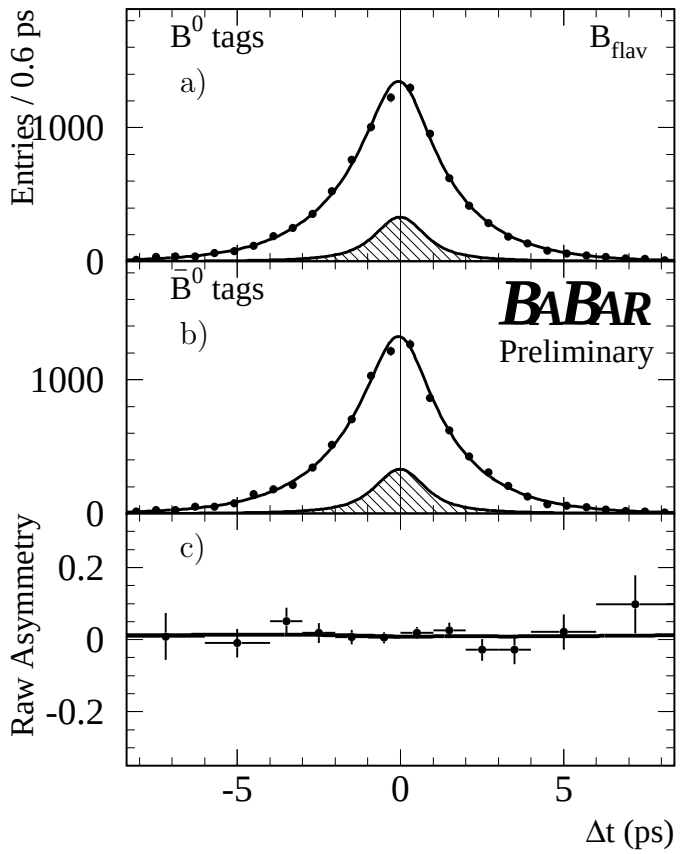

FIG. 3: Number of $B_{\rm flav}$ candidates in the signal region a) with a B^0 tag, N_{B^0}, and b) with a $\overline{B}^0$ tag, $N_{\overline{B}^0}$, and c) the raw asymmetry $(N_{B^0} - N_{\overline{B}^0})/(N_{B^0} + N_{\overline{B}^0})$, as functions of Δt. The solid curves represent the result of the combined fit to all selected $B_{\rm flav}$ events. The shaded regions represent the background contributions.

We are grateful for the extraordinary contributions of our PEP-II colleagues in achieving the excellent luminosity and machine conditions that have made this work possible. The success of this project also relies critically on the expertise and dedication of the computing organizations that support *BABAR*. The collaborating institutions wish to thank SLAC for its support and the kind hospitality extended to them. This work is supported by the US Department of Energy and National Science Foundation, the Natural Sciences and Engineering Research Council (Canada), Institute of High Energy Physics (China), the Commissariat à l'Energie Atomique and Institut National de Physique Nucléaire et de Physique des Particules (France), the Bundesministerium für Bildung und Forschung (Germany), the Istituto Nazionale di Fisica Nucleare (Italy), the Research Council of Norway, the Ministry of Science and Technology of the Russian Federation, and the Particle Physics and Astronomy Research Council (United Kingdom). Individuals have received support from the A. P. Sloan Foundation, the Research Corporation, and the Alexander von Humboldt Foundation.

APPENDIX A: TIME-DEPENDENT *CP* ASYMMETRY IN $B \to J/\psi K^{*0}(K^{*0} \to K^0_S\pi^0)$

The decay $B \to J/\psi K^*$ is described by three amplitudes. In the transversity basis [15, 16], the amplitudes A_0, $A_\parallel$ and $A_\perp$ have *CP* eigenvalues $+1, +1$ and -1, respectively. A_0 corresponds to longitudinal polarization of the vector mesons, and $A_\parallel$ and $A_\perp$ correspond to parallel and perpendicular transverse polarizations, respectively. The relative phase between the parallel (perpendicular) transverse amplitude and the longitudinal amplitude is given by $\phi_\parallel \equiv \arg(A_\parallel/A_0)$ ($\phi_\perp \equiv \arg(A_\perp/A_0)$). The transversity frame is defined as the J/ψ rest frame (see Fig. 4). The K^* direction defines the negative x axis. The $K\pi$ decay plane defines the (x, y) plane, with y oriented such that $p_y(K) > 0$. The z axis is the normal to this plane, and the coordinate system is right-handed. The transversity angles

θ_{tr} and φ_{tr} are defined as the polar and azimuthal angles of the positive lepton from the J/ψ decay; θ_{K^*} is the K^* helicity angle defined in the K^* rest frame as the angle between the K direction and the direction opposite to the J/ψ.

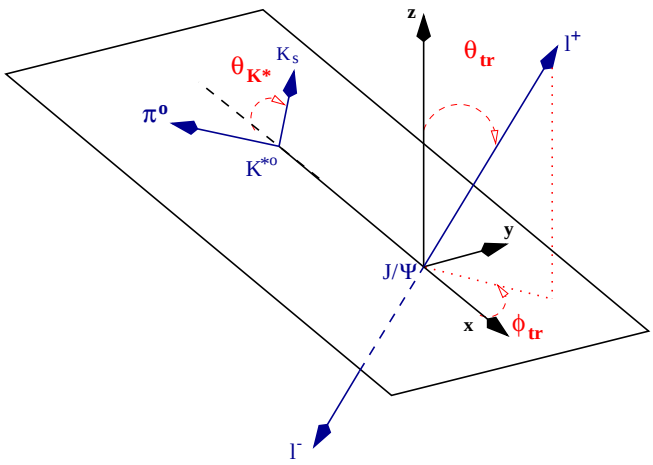

FIG. 4: Definitions of transversity angles θ_{tr}, φ_{tr}, and θ_{K^*}. The angles θ_{tr} and φ_{tr} are determined in the J/ψ rest frame. The angle θ_{K^*} is determined in the K^* rest frame.

The time- and transversity-angle-dependent decay rate distributions $\mathrm{f}_+(\mathrm{f}_-)$ when the tagging meson is a $B^0(\overline{B}^0)$ are given by

$$\begin{aligned}\mathrm{f}_\pm(\Delta t,\vec{\omega}) &= \frac{e^{-|\Delta t|/\tau_{B^0}}}{4\tau_{B^0}}\Big[I(\vec{\omega};\vec{\mathcal{A}}) \mp \Big\{C(\vec{\omega};\vec{\mathcal{A}})\cos(\Delta m_d\Delta t) \\ &\quad + \Big[S_{\sin2\beta}(\vec{\omega};\vec{\mathcal{A}})\sin2\beta + S_{\cos2\beta}(\vec{\omega};\vec{\mathcal{A}})\cos2\beta\Big]\sin(\Delta m_d\Delta t)\Big\}\Big]. \qquad \text{(A1)}\end{aligned}$$

The coefficients I, C, $S_{\sin2\beta}$, and $S_{\cos2\beta}$, which depend on the transversity angles $\vec{\omega} = (\theta_{K^*}, \theta_{tr}, \varphi_{tr})$ and the transversity amplitudes $\vec{\mathcal{A}} = (A_0, A_\parallel, A_\perp)$, are given by

$$\begin{aligned}I(\vec{\omega};\vec{\mathcal{A}}) &= f_1(\vec{\omega})|A_0|^2 + f_2(\vec{\omega})|A_\parallel|^2 + f_3(\vec{\omega})|A_\perp|^2 + f_5(\vec{\omega})|A_\parallel||A_0|\cos(\phi_\parallel - \phi_0) \\ C(\vec{\omega};\vec{\mathcal{A}}) &= f_4(\vec{\omega})|A_\parallel||A_\perp|\sin(\phi_\perp - \phi_\parallel) + f_6(\vec{\omega})|A_\perp||A_0|\sin(\phi_\perp - \phi_0) \\ S_{\sin2\beta}(\vec{\omega};\vec{\mathcal{A}}) &= f_1(\vec{\omega})|A_0|^2 + f_2(\vec{\omega})|A_\parallel|^2 - f_3(\vec{\omega})|A_\perp|^2 + f_5(\vec{\omega})|A_\parallel||A_0|\cos(\phi_\parallel - \phi_0) \\ S_{\cos2\beta}(\vec{\omega};\vec{\mathcal{A}}) &= -f_4(\vec{\omega})|A_\parallel||A_\perp|\cos(\phi_\perp - \phi_\parallel) - f_6(\vec{\omega})|A_\perp||A_0|\cos(\phi_\perp - \phi_0) \qquad \text{(A2)}\end{aligned}$$

with

$$\begin{aligned}f_1(\vec{\omega}) &= \frac{9}{32\pi}2\cos^2(\theta_{K^*})\left[1 - \sin^2(\theta_{tr})\cos^2(\varphi_{tr})\right] \\ f_2(\vec{\omega}) &= \frac{9}{32\pi}\sin^2(\theta_{K^*})\left[1 - \sin^2(\theta_{tr})\sin^2(\varphi_{tr})\right] \\ f_3(\vec{\omega}) &= \frac{9}{32\pi}\sin^2(\theta_{K^*})\sin^2(\theta_{tr}) \\ f_4(\vec{\omega}) &= \frac{9}{32\pi}\sin^2(\theta_{K^*})\sin(2\theta_{tr})\sin(\varphi_{tr}) \\ f_5(\vec{\omega}) &= -\frac{9}{32\pi}\frac{1}{\sqrt{2}}\sin(2\theta_{K^*})\sin^2(\theta_{tr})\sin(2\varphi_{tr}) \\ f_6(\vec{\omega}) &= \frac{9}{32\pi}\frac{1}{\sqrt{2}}\sin(2\theta_{K^*})\sin(2\theta_{tr})\cos(\varphi_{tr}). \qquad \text{(A3)}\end{aligned}$$

[1] N. Cabibbo, Phys. Rev. Lett. **10**, 531 (1963);
M. Kobayashi and T. Maskawa, Prog. Th. Phys. **49**, 652 (1973).
[2] A.B. Carter and A.I. Sanda, Phys. Rev. **D23**, 1567 (1981);
I.I. Bigi and A.I. Sanda, Nucl. Phys. **B193**, 85 (1981).
[3] *BABAR* Collaboration, B. Aubert *et al.*, Phys. Rev. Lett. **87**, 091801 (2001).
[4] BELLE Collaboration, K. Abe *et al.*, Phys. Rev. Lett. **87**, 091802 (2001).
[5] OPAL Collaboration, K. Ackerstaff *et al.*, Eur. Phys. Jour. C **5**, 379 (1998);
CDF Collaboration, T. Affolder *et al.*, Phys. Rev. **D61**, 072005 (2000);
ALEPH Collaboration, R. Barate *et al.*, Phys. Lett. **B492**, 259 (2000);
BABAR Collaboration, B. Aubert *et al.*, Phys. Rev. Lett. **86**, 2515 (2001);
BELLE Collaboration, A. Abashian *et al.*, Phys. Rev. Lett. **86**, 2509 (2001).
[6] *BABAR* Collaboration, B. Aubert *et al.*, *BABAR*-PUB-01/03, SLAC-PUB-9060, hep-ex/0201020,
submitted to Phys. Rev. D .
[7] *BABAR* Collaboration, B. Aubert *et al.*, Nucl. Instr. and Methods **A479**, 117 (2002).
[8] `http://wwwinfo.cern.ch/asd/geant4/geant4.html`
[9] See, for example, L. Wolfenstein, Eur. Phys. Jour. C **15**, 115 (2000).
[10] *BABAR* Collaboration, B. Aubert *et al.*, Phys. Rev. Lett. **87**, 241801 (2001).
[11] A.S. Dighe, I. Dunietz and R. Fleischer, Phys. Lett. **B433**, 147 (1998).
[12] Particle Data Group, D.E. Groom *et al.*, Eur. Phys. Jour. C **15**, 1 (2000).
[13] M. Suzuki, Phys. Rev. **D64**, 117503 (2001).
[14] See, for example, F.J. Gilman, K. Kleinknecht and B. Renk, Eur. Phys. Jour. C **15**, 110 (2000).
[15] I. Dunietz, H.R. Quinn, A. Snyder, W. Toki and H. J. Lipkin, Phys. Rev. D **43**, 2193 (1991).
[16] A.S. Dighe, I. Dunietz, H.J. Lipkin and J.L. Rosner, Phys. Lett. B**369**, 144 (1996).